DOT/FAA/TC-16/24

Federal Aviation Administration
William J. Hughes Technical Center
Aviation Research Division
Atlantic City International Airport
New Jersey 08405

Abusive Testing of Proton Exchange Membrane Hydrogen Fuel Cells

October 2016

Final Report

U.S. Department of Transportation
Federal Aviation Administration

NOTICE

Technical Report Documentation Page

1. Report No.	2. Government Accession No.	3. Recipient's Catalog No.
DOT/FAA/TC-16/24		

4. Title and Subtitle	5. Report Date
ABUSIVE TESTING OF PROTON EXCHANGE MEMBRANE HYDROGEN FUEL CELLS	October 2016
	6. Performing Organization Code
7. Author(s)	8. Performing Organization Report No.
Steven M. Summer[1] and Shane Nicholson[2]	
9. Performing Organization Name and Address	10. Work Unit No. (TRAIS)
[1]Federal Aviation Administration William J. Hughes Technical Center Aviation Research Division Fire Safety Branch, ANG-E21 Atlantic City International Airport, NJ 08405 [2]Parker Hannifin Corporation Aerospace Group Central Engineering FDC 6500 West Freeway, Suite 1010 Fort Worth, TX 76116	
	11. Contract or Grant No.
12. Sponsoring Agency Name and Address	13. Type of Report and Period Covered
FAA Northwest Mountain Regional Transport Airplane Directorate 1601 Lind Ave SW Renton, WA 98057	Final Report
	14. Sponsoring Agency Code
	ANM-111

15. Supplementary Notes

16. Abstract

In collaboration with Parker Hannifin Corporation, the Fire Safety Branch of the FAA conducted testing to evaluate the effects of three potential failure conditions of hydrogen proton exchange (or polymer electrolyte) membrane fuel cell stacks supplied by Nuvera Fuel Cells. The three conditions examined were a loss of coolant to the stack, short circuit, and a crossflow condition. The testing showed that the stacks were extremely robust under a variety of failure conditions and that, with proper monitoring of key variables, the failures could have been detected and flow of reactant gases stopped prior to any hazardous effects occurring.

It is recommended that any installation of a hydrogen fuel cell system ensure that reactant supply gas pressures, stack temperatures, coolant temperatures, and stack electrical load characteristics be adequately monitored and connected to system shutdown features. In addition, provisions should be made so that the surrounding environment is monitored for any temperature or hydrogen gas concentration increases.

17. Key Words	18. Distribution Statement
Hydrogen, Fuel cell, Proton exchange membrane, PEM	This document is available to the U.S. public through the National Technical Information Service (NTIS), Springfield, Virginia 22161. This document is also available from the Federal Aviation Administration William J. Hughes Technical Center at actlibrary.tc.faa.gov.

19. Security Classif. (of this report)	20. Security Classif. (of this page)	21. No. of Pages	22. Price
Unclassified	Unclassified	34	

TABLE OF CONTENTS

LIST OF FIGURES

LIST OF ACRONYMS

ARC	Aviation Rulemaking Committee
DAS	Data acquisition system
ODA	Oxygen-depleted air
MEA	Membrane electrode assembly
PEM	Proton exchange (or polymer electrolyte) membrane
THC	Total hydrocarbon

EXECUTIVE SUMMARY

Driven by increasingly stringent environmental regulations, the aviation community is exploring new integrated and greener technologies to satisfy aircraft power and electrical needs. Hydrogen-based fuel cells are one such technology that is attractive to the aviation community because of their high power output, efficiency, and environmental friendliness as compared to fossil fuels. The aviation industry has been evaluating and developing prototypes to support a variety of operations onboard the aircraft. These operations range from replacing the airplane's main battery, ram air turbine, or even the auxiliary power unit to supplying power to galley cooking equipment. In addition to the electrical power supply, industry is evaluating potential ways to use the byproducts of hydrogen-based fuel cells, water, and oxygen-depleted air. These byproducts could be used for fuel tank inerting, cargo bay fire suppression, or water supply.

In collaboration with Parker Hannifin Corporation, the Fire Safety Branch of the FAA conducted testing to evaluate the effects of three potential failure conditions of hydrogen proton exchange (or polymer electrolyte) membrane fuel cell stacks supplied by Nuvera Fuel Cells. The three conditions examined were a loss of coolant to the stack, short circuit, and a crossflow condition. After exposing the stack to the various failure conditions, it was observed that the stack continued to operate for an extended period of time before any hazardous effects were observed. Once the stack components failed, external heat in excess of the normal operational temperature was observed; however, only the loss of coolant and crossflow tests resulted in any fire/sparking from the test unit. In addition, the crossflow condition test resulted in some hydrogen leakage into the surrounding pressure vessel.

There were various opportunities for detection of the failure during the time spanning from when the failure event was initiated to when the stack deteriorated to the point of flaming/sparking. Failure detection could have been achieved by monitoring the reactant gas supply pressures, coolant exit temperatures, stack surface temperatures, or the stack output voltage and current.

The testing showed that the stacks were extremely robust under a variety of failure conditions and that, with proper monitoring of key variables, the failures could have been detected and flow of reactant gases stopped prior to any hazardous effects occurring. It is recommended that any installation of a hydrogen fuel cell system ensure that reactant supply gas pressures, stack temperatures, coolant temperatures, and stack electrical load characteristics be adequately monitored and connected to system shutdown features. In addition, provisions should be made so that the surrounding environment is monitored for any temperature or hydrogen gas concentration increases.

It should be noted that this testing only evaluated failure mechanisms of the fuel cell stack itself. The storage and distribution of high-pressure hydrogen gas provides its own level of hazard that also needs to be addressed. Further testing of other hydrogen fuel cells, with a focus on these aspects, should be conducted and evaluated prior to any implementation of a fuel cell system to ensure that any safety issues are being adequately addressed.

1. INTRODUCTION

1.1 BACKGROUND

Driven by increasingly stringent environmental regulations, the aviation community is exploring new integrated and greener technologies to satisfy aircraft power and electrical needs. Hydrogen-based fuel cells, attractive to the aviation community because of their high power output, efficiency, and environmental friendliness as compared to fossil fuels, are one such technology. The aviation industry has been evaluating and developing prototypes to support a variety of onboard operations. These operations range from replacing the airplane's main battery, ram air turbine, or even the auxiliary power unit to supplying power to galley cooking equipment. In addition to the electrical power supply, industry is evaluating potential ways to use the byproducts of hydrogen-based fuel cells, water, and oxygen-depleted air (ODA). These byproducts could be used for fuel-tank inerting, cargo bay fire suppressionn, or water supply.

The implementation of hydrogen-based fuel cells on commercial aircraft, however, presents a number of safety concerns because of the highly flammable nature of hydrogen gas. Industry has been working to address these concerns through a joint European Organization for Civil Aviation Equipment/Society of Automotive Engineers committee (AE-7AFC) to develop testing standards and installation guidance for proton exchange (or polymer electrolyte) membrane (PEM) fuel cells. In addition, the FAA recently formed an Energy Storage Device Aviation Rulemaking Committee (ARC) to, among other things, determine the hazards and applicable airworthiness requirements concerning the use of hydrogen-based fuel cells on transport-category aircraft.

There are several types of hydrogen-based fuel cells, including PEM, alkaline, solid oxide, and others. The data generated in this report used a PEM fuel cell stack. PEM fuel cells are the focus of the AE-7AFC committee and one of the focal points of the FAA ARC.

The PEM fuel cell transforms the chemical energy resulting from the electrochemical reaction of hydrogen and oxygen into electrical energy. A diagram of a typical PEM membrane electrode assembly (MEA) is shown in figure 1. A fuel cell stack is constructed of multiple layers of these MEAs separated by bipolar plates. Hydrogen is supplied to the anode, whereas air, or pure oxygen, is supplied to the cathode. The hydrogen is separated into protons and electrons through a platinum catalyst. The hydrogen protons then migrate through the PEM to the cathode side while the electrons travel along an external load circuit to the cathode side, thereby generating the current output of the fuel cell. The oxygen then reacts with the hydrogen protons, thereby generating water, ODA, and heat.

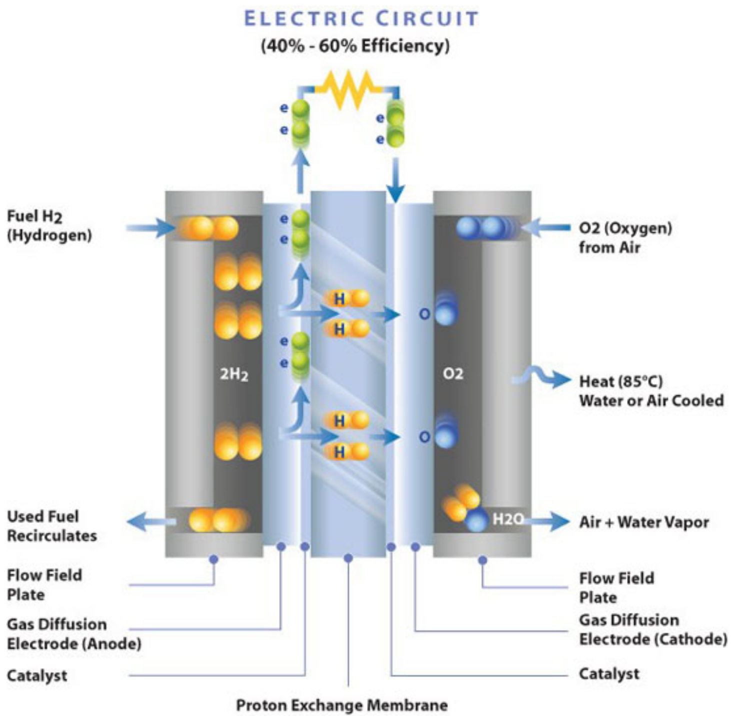

Figure 1. Diagram of a typical proton exchange membrane fuel cell [1]

Because of the flammable nature of hydrogen, a failure within the fuel cell could potentially result in hazardous conditions. Potential failure mechanisms include a short circuit of the fuel cell, a crossflow condition in which the anode and cathode react with each other or an overheat condition within the fuel cell.

1.2 SCOPE OF EXPERIMENTS

The objective of this study was to evaluate potential failure conditions within a PEM fuel cell stack. Conditions examined included a short circuit, crossflow, and a loss of coolant event. The effects of each failure and the potential for indication prior to failure through a variety of measured parameters were examined.

2. EXPERIMENTAL APPARATUS

The experiments discussed within this report were conducted at the FAA William J. Hughes Technical Center within the Pressure Fire Modeling Facility. This facility houses a 10-m3 vessel capable of withstanding a maximum working pressure of 650 psi. The fuel cell stack, along with temperature and gas measurement probes, was situated inside this pressure vessel. High-speed and infrared cameras were used to record the test events. The fuel cell stack was connected to an external load bank and supplied with dry hydrogen and oxygen gases and deionized water as a coolant source. In addition, gas analyzers were used to measure oxygen, carbon monoxide, carbon dioxide, hydrogen, and total hydrocarbon (THC) concentration within the pressure chamber. Figure 2 is a photograph of the pressure vessel, and figure 3 shows a schematic of the overall test setup. Figure 4 is a photograph of the test setup with various items of interest labeled for reference.

Figure 2. Pressure vessel located at the FAA's Pressure Fire Modeling Facility

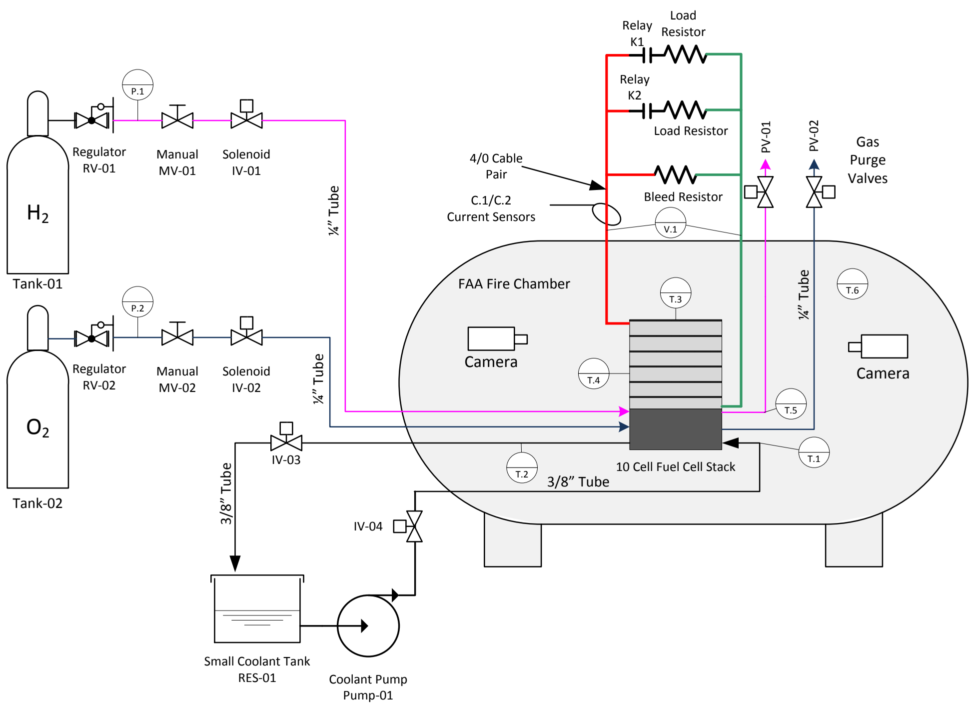

Figure 3. Schematic of overall test setup

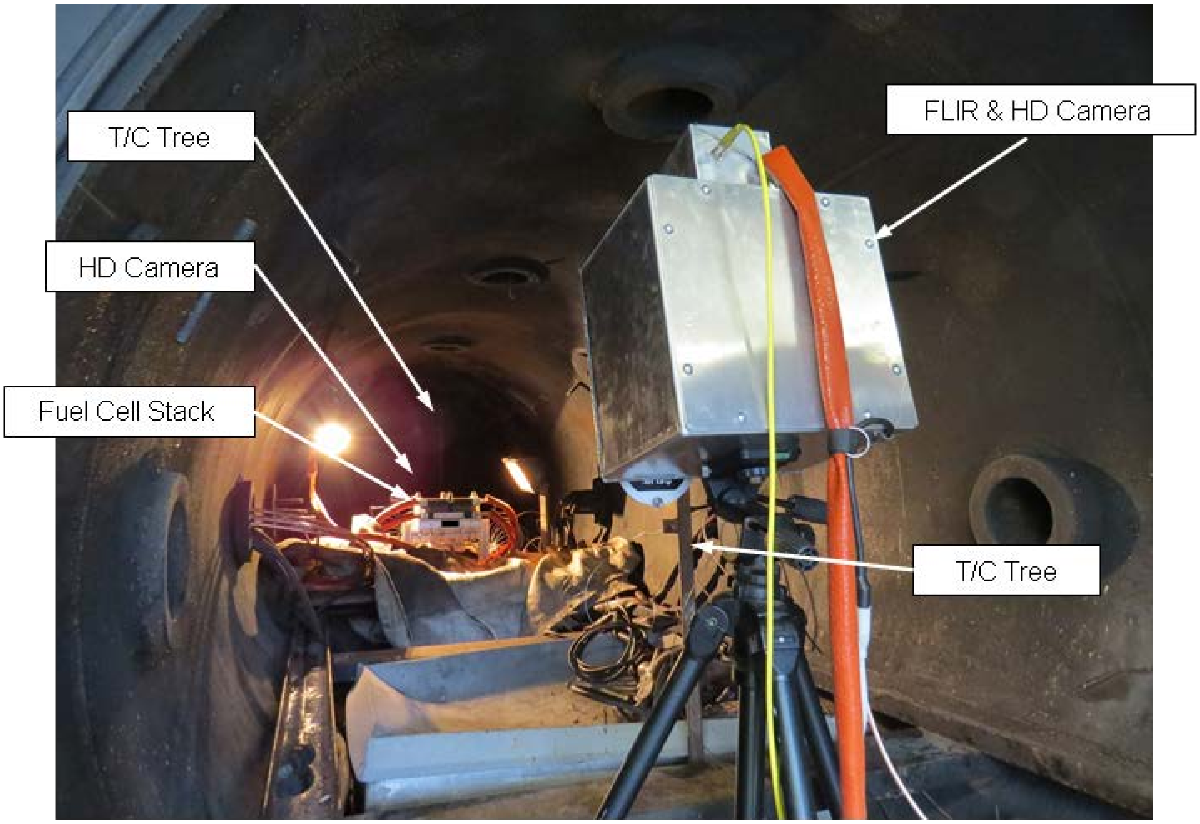

Figure 4. Photograph of experimental setup

2.1 FUEL CELL STACKS

Three fuel cell stacks were used for testing. Figure 5 is a photograph of one of them, as set up for testing, and figure 6 shows the placement of the surface thermocouples. These were PEM-type fuel cell stacks with metal bipolar plates, consisting of 10 cells with an active area of 250 cm^2 and laboratory-grade configuration hardware. An adapter manifold with silicon gaskets was used to interface with the reactant and coolant inputs and outputs of the fuel cell. These fuel cells were basic research stacks with no protective covers or electrical isolation, with the manifold end acting as the ground reference for the stack. The opposite end of the stack was electrically charged when reactants were present.

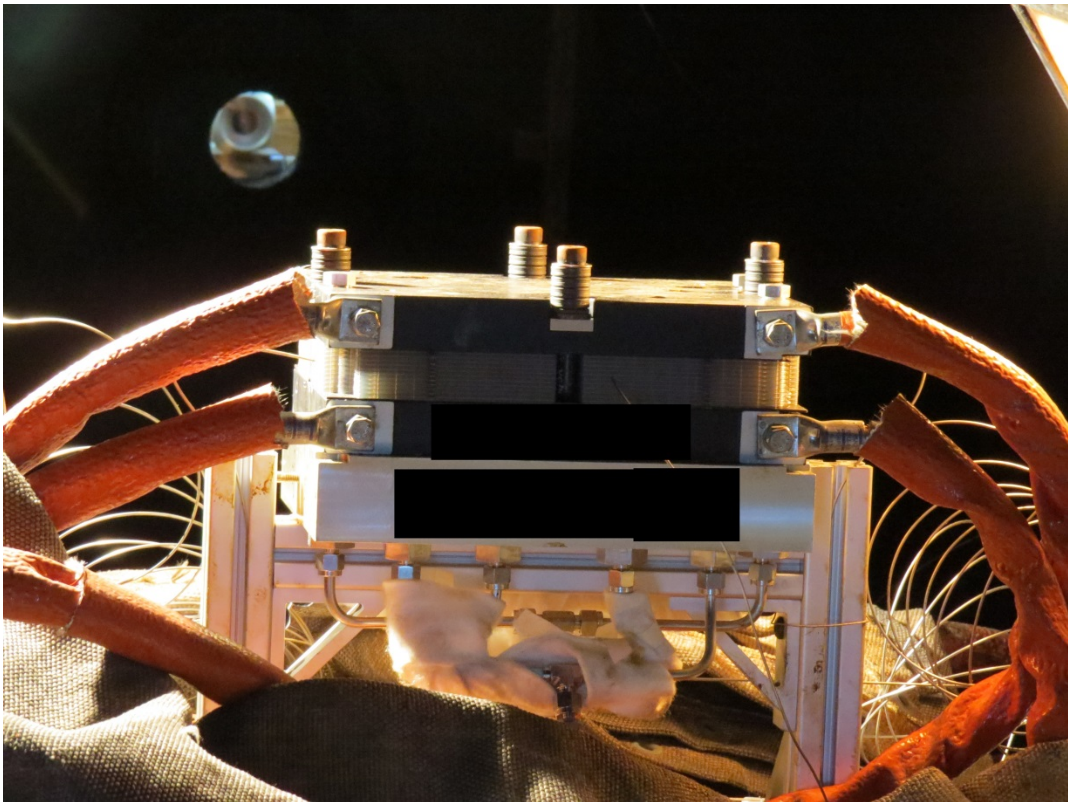

Figure 5. Photograph of fuel cell stack as used in experiments

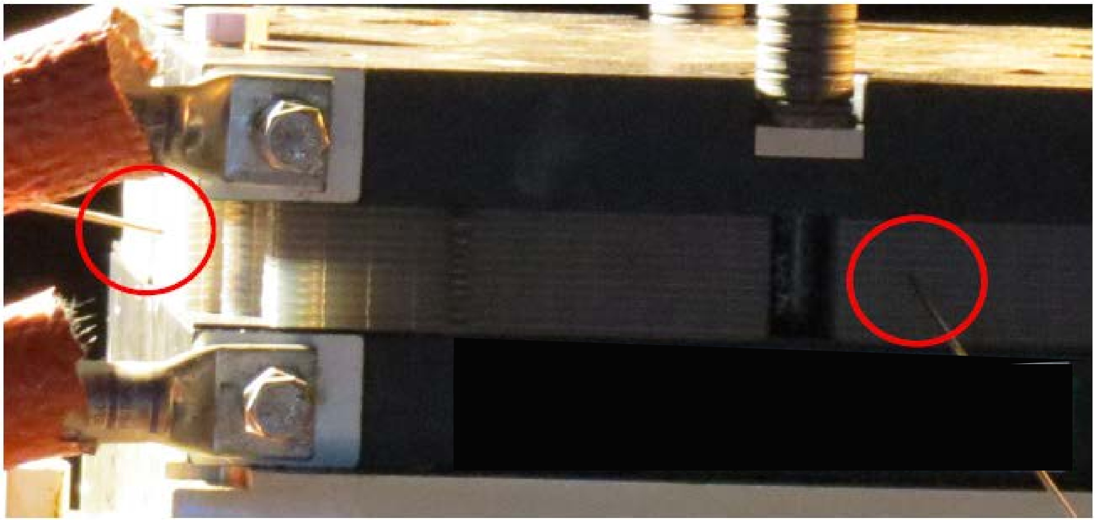

Figure 6. Photograph showing placement of surface thermocouples on fuel cell stack

2.2 ANODE AND CATHODE GAS SUPPLY

Dry gases of O_2 (at 99% purity) and H_2 (at 99.999% purity) were supplied to the cathode and anode sides, respectively. Pure O_2 was used as opposed to air on the cathode side so as to maximize the potential fire load; however, it should be noted that the fuel stacks used were designed for use with air, not pure O_2. The gas supply was controlled via manual needle valves on the outlet of the gas bottles to achieve the desired pressures, and electrically controlled solenoid valves were used to turn the gas flow on and off as needed. The reactant gases were supplied to the test unit through 3/8″ copper tubing.

2.3 COOLANT SUPPLY

Coolant flow was supplied to the fuel cell stack through a 1.7 gpm pump connected to a 2-gallon supply of deionized water that was recirculated through the system during the test. Control of the flow was via a pair of electrically controlled solenoid valves. The coolant was supplied to the test unit through 3/8″ stainless steel tubing.

2.4 LOAD BANK

The electrical load was applied to the fuel cell using a load bank, shown in figure 7, consisting of two 525A stainless steel ribbon resistors with a resistance of 0.02 ohms each. These were combined in series, providing 0.04 ohms total resistance for the loss of coolant test or in parallel to provide 0.01 ohms total resistance for the short-circuit test.

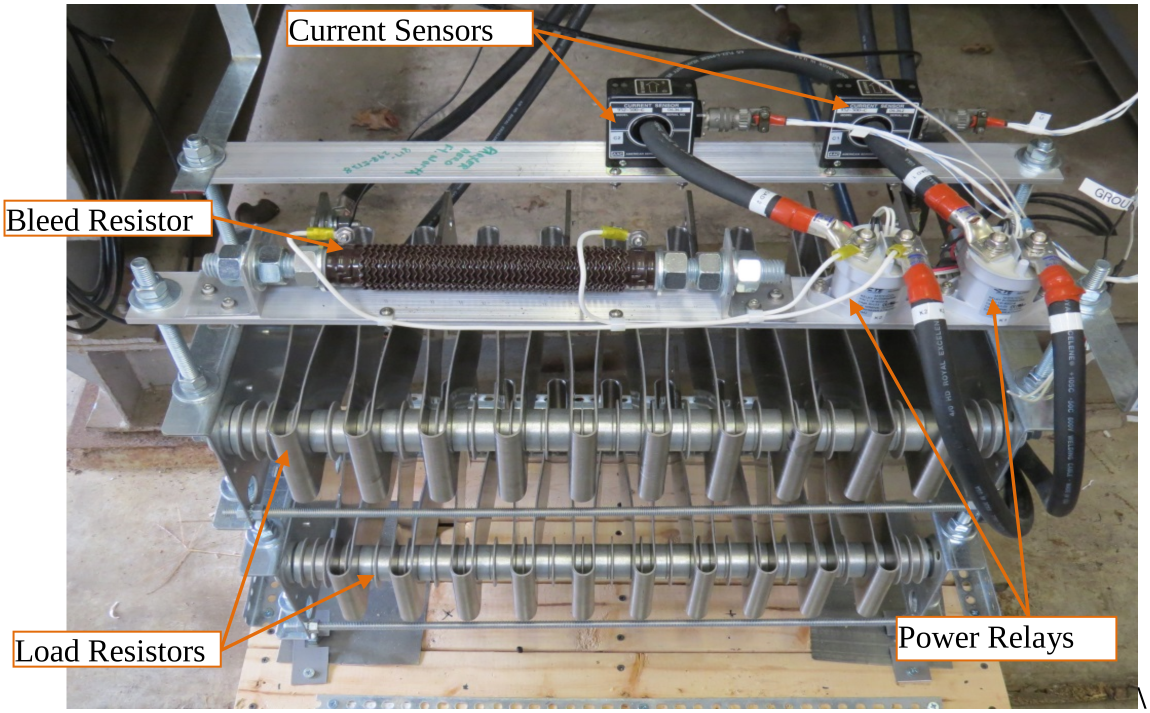

Figure 7. Photograph of the load bank installed for testing

In addition, a smaller bleed resistor was used to keep the fuel cell loaded at 15A during start up at no-load conditions so as to prevent the unit from operating at open circuit voltage. This resistor was rated at 0.5 ohm, 300W.

Two relays were used to direct the current through either the two ribbon resistors or the bleed resistor. Current output was measured through the use of two current sensors, with a range from

0–500A and accuracy of ±0.4%. Voltage output was measured directly through the data acquisition system (DAS).

2.5 TEMPERATURE MEASUREMENT

Temperature measurements were recorded with 1/8″ sheathed K-type thermocouples. Measurements were taken of the coolant supply and exit temperatures and on each side of the fuel cell stack. The stack thermocouples were each placed at the approximate center of the MEA stacks on the front, rear, left, and right sides. In addition, five thermocouples situated on existing thermocouple trees were used to monitor and record the chamber temperature.

2.6 GAS MEASUREMENT

Gas measurements of CO, CO_2, O_2, H_2, and THC were monitored throughout testing. CO, CO_2, and O_2 were all measured with a Rosemount Analytical MLT-4 multi-gas analyzer; an H2scan HY-OPTIMA™ 2700 and a Signal Instruments 3000HM analyzer were used for H_2 and THC measurements, respectively. THC samples were routed from the pressure chamber to the analyzer with heated lines maintained at 200°F so as to ensure there was no condensation of the sample prior to reaching the sensor.

3. EXPERIMENTAL PROCEDURES

Prior to each test, leak checks of the anode and cathode lines were conducted using nitrogen gas. In addition, leak checks of the coolant path were conducted. The DAS was initiated and all sensors were checked for proper functionality. The coolant flow was initiated and H_2 and O_2 gas bottle pressures were set at 36.3 and 34.8 psia, respectively. With the test article at ambient temperature conditions, valves were opened to allow the anode and cathode gases to flow. The unit was then run at this idle condition for a period of time to ensure proper operation of the fuel cell and all measurement apparatuses prior to proceeding with the test conditions.

3.1 LOSS OF COOLANT TEST

The load bank relays were closed to move the unit from idle to a power supply condition. This produced an approximate 170A load on the fuel cell system. The system was maintained at this condition for a period of time before shutting down the flow of coolant to the fuel cell stack. This was achieved by turning off the coolant pump and closing the coolant isolation valves. Data and video recording were then continued until a failure event occurred.

3.2 SHORT-CIRCUIT TEST

Prior to the short-circuit test, the load bank was reconfigured such that the load resistors were parallel with the bleed resistor. Once the test was underway, the load bank relays were closed when the fuel cell system was operating at the idle condition, thereby inducing a load of approximately 470A on the system. The system was maintained at this condition, with data collection and video recording continuing until a failure event occurred.

3.3 CROSSFLOW TEST

Pretest inspections of the final fuel cell stack verified an internal failure condition within the fuel cell stack, which led to a crossflow condition whereby the H_2, once introduced to the fuel cell stack, was interacting with the O_2. The stack was run in its idle condition and a short-circuit condition to examine any potential failure events resulting from this crossflow condition.

4. DISCUSSION OF RESULTS

Experimental data and results of the post-test teardown analysis of each of the fuel cell stacks are provided in this section. On each of the data plots provided, significant events relevant to the test are labeled. The various gas analysis probes did not provide any substantial measurements, indicating an inconsequential change in quantities of CO, CO_2, O_2, THC, and H_2 for each of the tests. As such, the gas analysis data from these experiments are not provided in this report.

4.1 LOSS OF COOLANT TEST

Figures 8–11 show the results of the loss of coolant test. Figure 8 shows a plot of the stack voltage and current along with the supply H_2 and O_2 pressures for the loss of coolant test. Figure 9 provides the four stack surface temperatures. Figure 10 shows the coolant supply and exit temperatures, and figure 11 shows the temperatures from the two temperature trees installed in the pressure vessel.

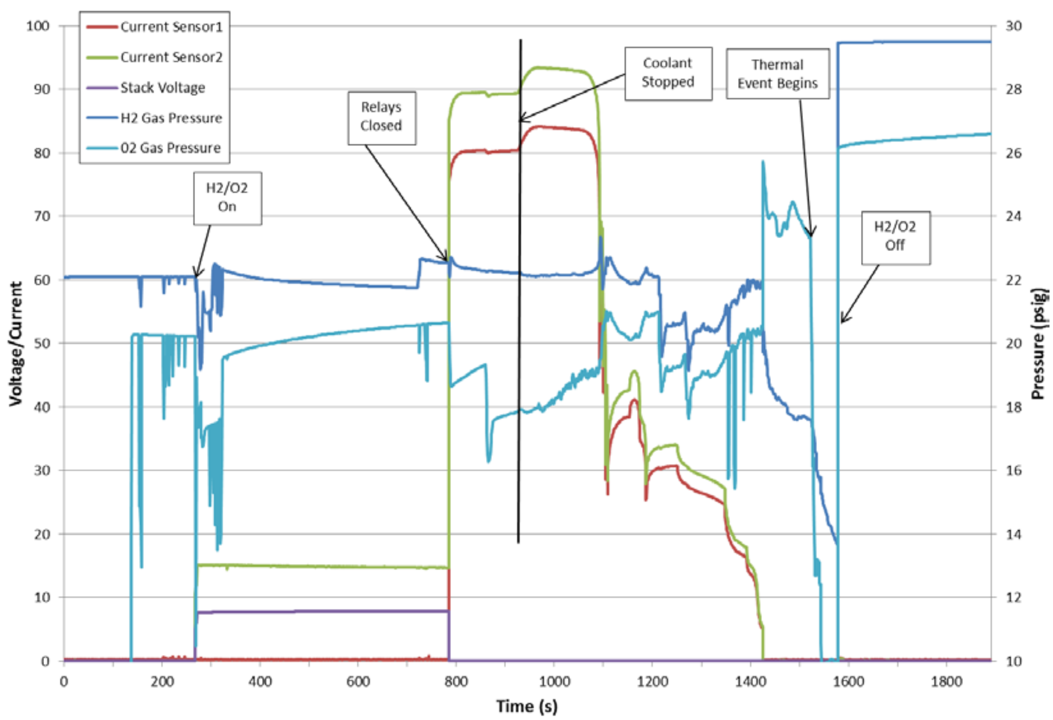

Figure 8. Loss of coolant test–reactant gas pressures and stack voltage/current

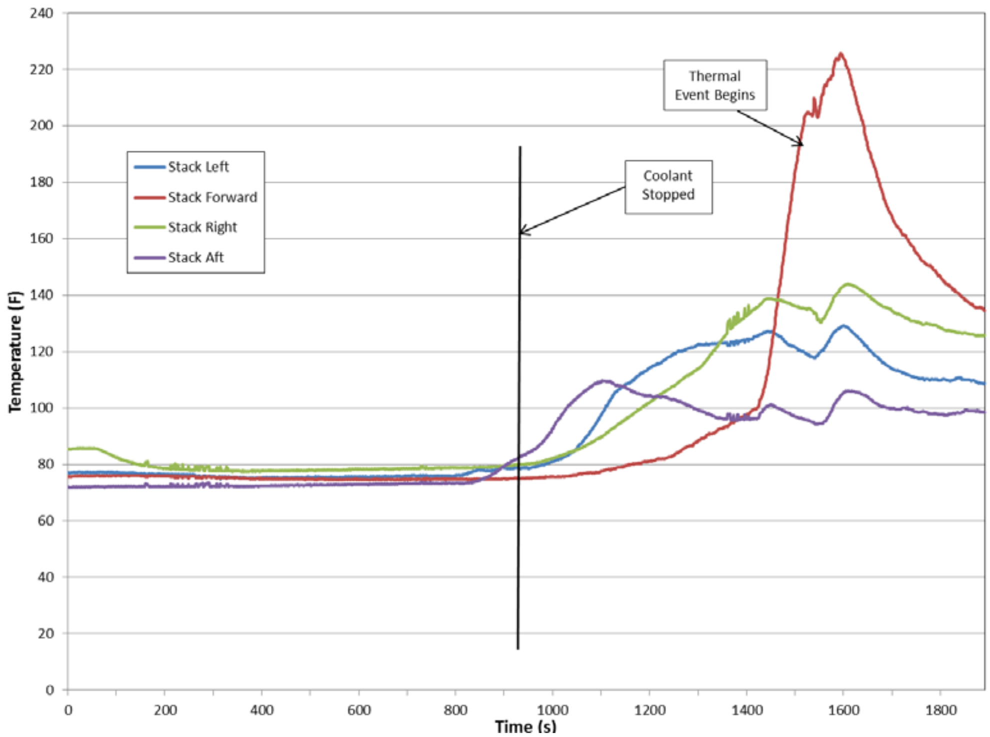

Figure 9. Loss of coolant test–stack surface temperatures

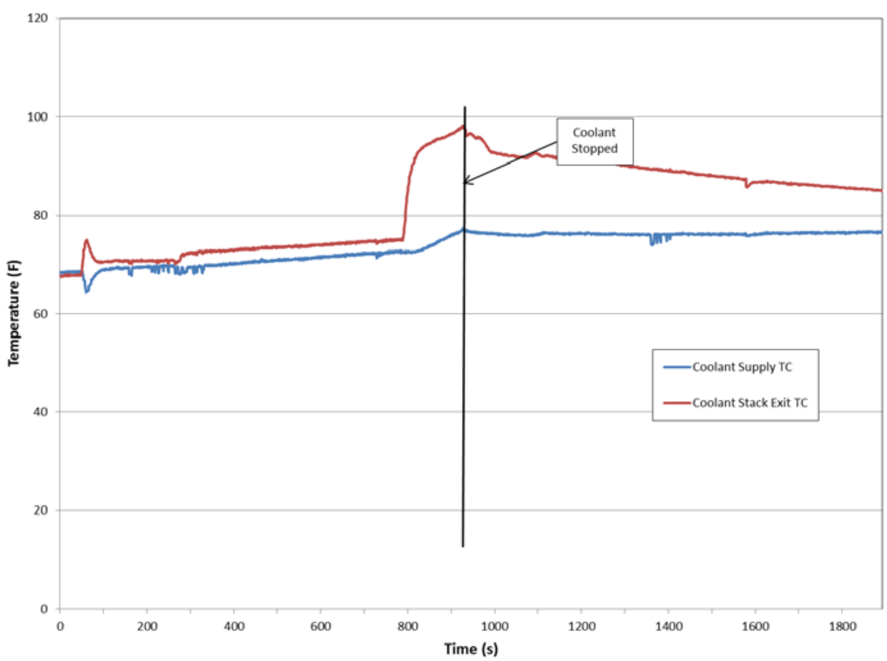

Figure 10. Loss of coolant test–coolant supply and exit temperatures

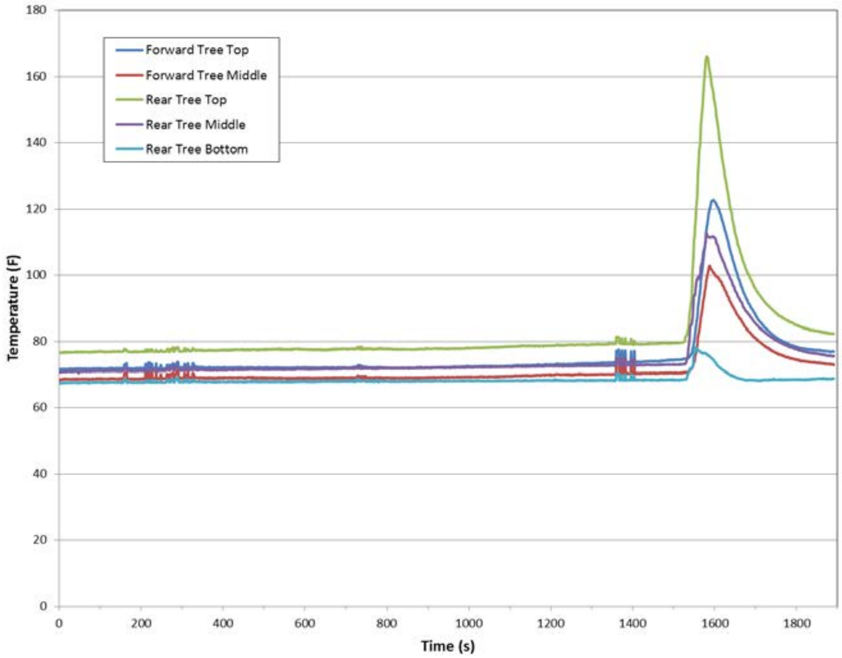

Figure 11. Loss of coolant test–pressure vessel temperatures

Once the electrical load was placed on the system, it was allowed to operate at 170A for approximately 140 seconds with coolant flow. At this point, the voltage reading was lost because of an error in the sensor placement. This sensor placement was corrected for subsequent tests. Following the initial load application, coolant flow to the unit was stopped by closing the coolant isolation valves and disabling the coolant pump. This resulted in a slight increase in the load current to approximately 175A for a period of 165 seconds. The current increase and a change in the coolant exit temperature were noted almost immediately after coolant flow was stopped. Within approximately 1 minute after stopping the coolant flow, an increase in the stack surface temperatures was also noted. In addition, at this point, current began to drop and reactant supply pressures were adjusted in an attempt to recover the unit. The current was unable to be fully recovered, however, and continued to decline until reaching 0A approximately 500 seconds after the coolant flow was stopped.

Approximately 111 seconds after completely losing current flow, a thermal event occurred, with sparks emanating from the forward-facing side of the fuel cell stack. This event is shown in figure 12 with a still frame from the recorded video of the test. The event is also shown in figures 9 and 11 as the forward stack surface temperature rises to over 220°F and all of the temperature probes within the pressure vessel also increase. The failure event was allowed to continue for approximately 1 minute after the sparking and flaming was observed. After this point, flow of the reactant gases was shut off and the primary fire was observed to self-extinguish within seconds. Burning of the fuel cell stack materials continued for approximately 40 seconds, after which time it self-extinguished.

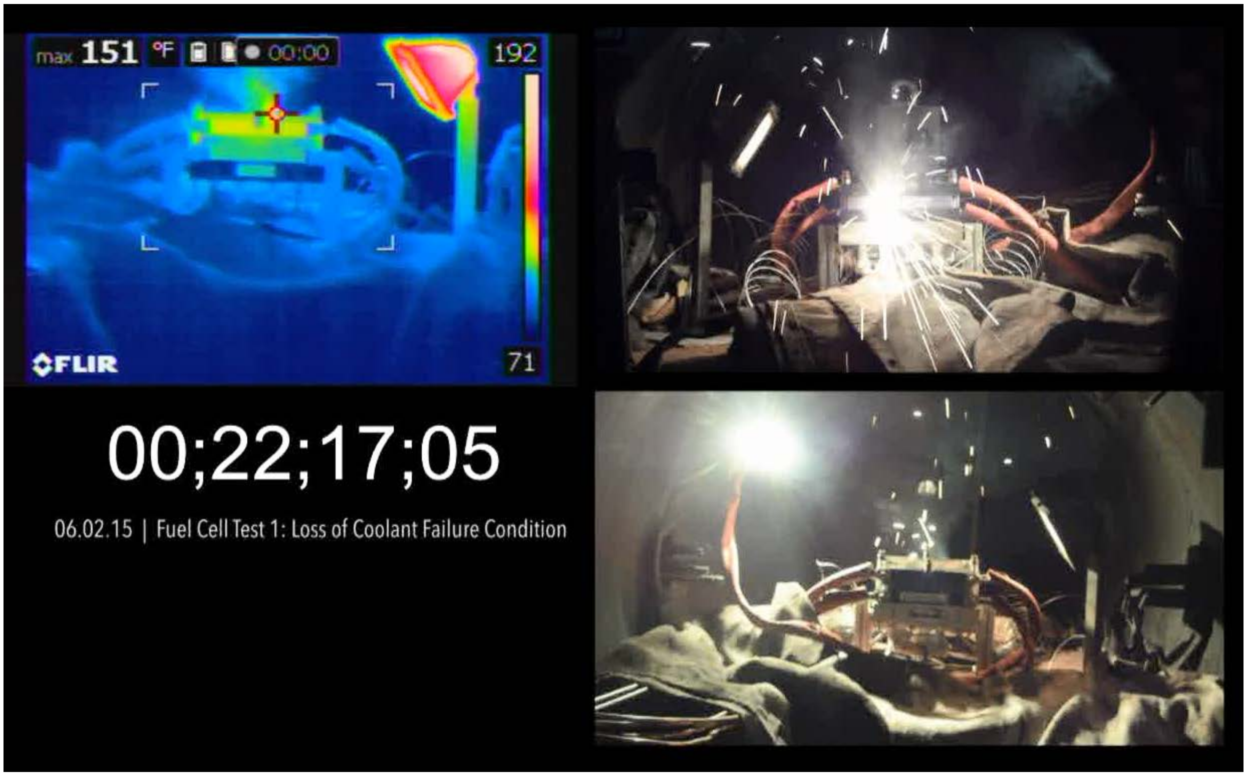

Figure 12. Loss of coolant test—still-frame photograph from test video during thermal event

Figures 13 and 14 are photographs of the unit after removal from the test fixture. Figure 13 is an external view of the forward side of the unit; it shows signs of severe damage to the O_2 inlet section of the stack. Figure 14 is a photograph, looking downward into the O_2 inlet port, with the gas manifold removed.

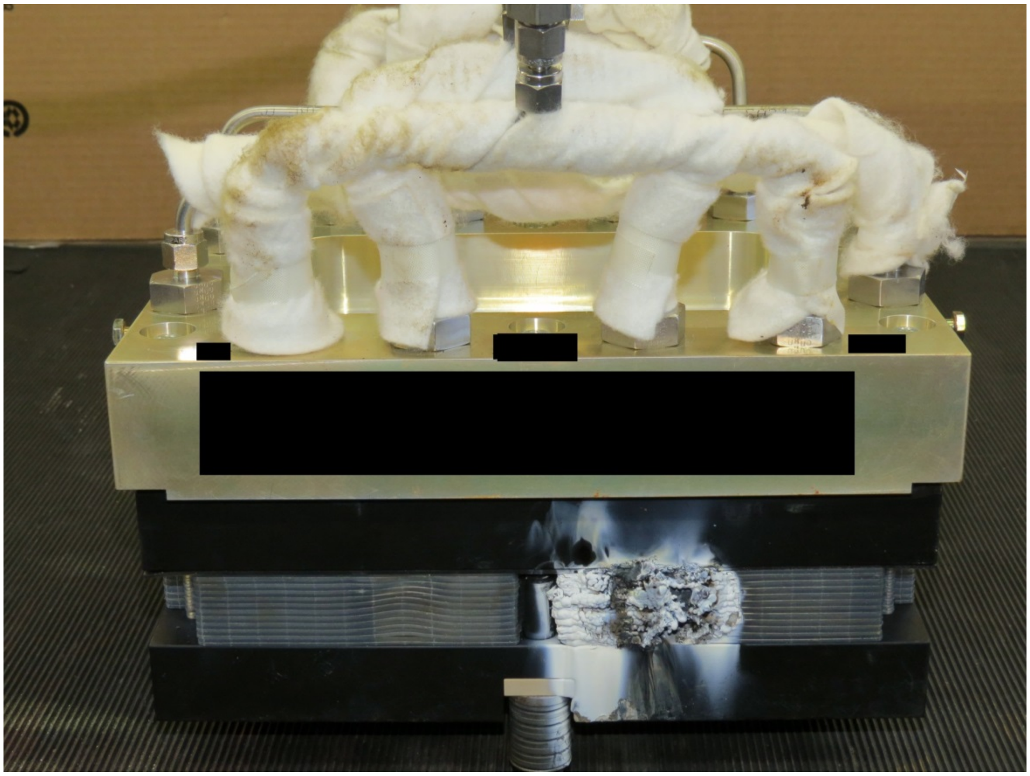

Figure 13. Loss of coolant test—post-test photograph of damaged area

Figure 14. Loss of coolant test—post-test photograph of cathode inlet port with gas manifold removed

A post-test teardown of the fuel cell stack, conducted by the manufacturer, revealed two distinct areas of damage. One, shown in figure 15, was situated between the active cell area at the oxidant and coolant inlet. This effectively was a hot spot where burning occurred on the active area of the bipolar metal plate. Damage was noted through the discoloration of the plate and fusing of the gasket material to the active area. The damage caused by this was most severe (i.e., largest damage area) toward the center of the stack and smaller toward the end cells. The burning caused by the failure in this area appeared to be caused by shorting of the plates and was isolated to the active area of the plates.

Figure 15. Loss of coolant test—photograph taken during post-test teardown of MEA active area damage (photograph intentionally blurred to protect proprietary information)

The second area of damage occurred outside of the active cell area between the anode outlet and the cathode inlet manifolds. This is the damage that was noted on the external photographs (see figures 13 and 14) immediately following the test. The post-test analysis showed that there was a fire at the cathode inlet that consumed the gasket material and a portion of the stainless steel plates in this area. This fire breached the anode outlet, allowing H_2 to continue to feed the fire. Figure 16 shows a close-up photograph of this area during the post-test disassembly of the fuel cell stack.

Figure 16. Loss of coolant test—photograph taken during post-test teardown of cathode inlet port damage (photograph intentionally blurred to protect proprietary information)

4.2 SHORT-CIRCUIT TEST

Figures 17–19 show the results of the short-circuit test. Figure 17 shows a plot of the stack voltage and current along with the supply H_2 and O_2 pressures for the loss of coolant test. Figure 18 shows the four stack surface temperatures, and figure 19 shows the coolant supply and exit temperatures. The temperature probes placed within the pressure vessel did not record any significant temperature events and, therefore, data from these probes are not provided in this report.

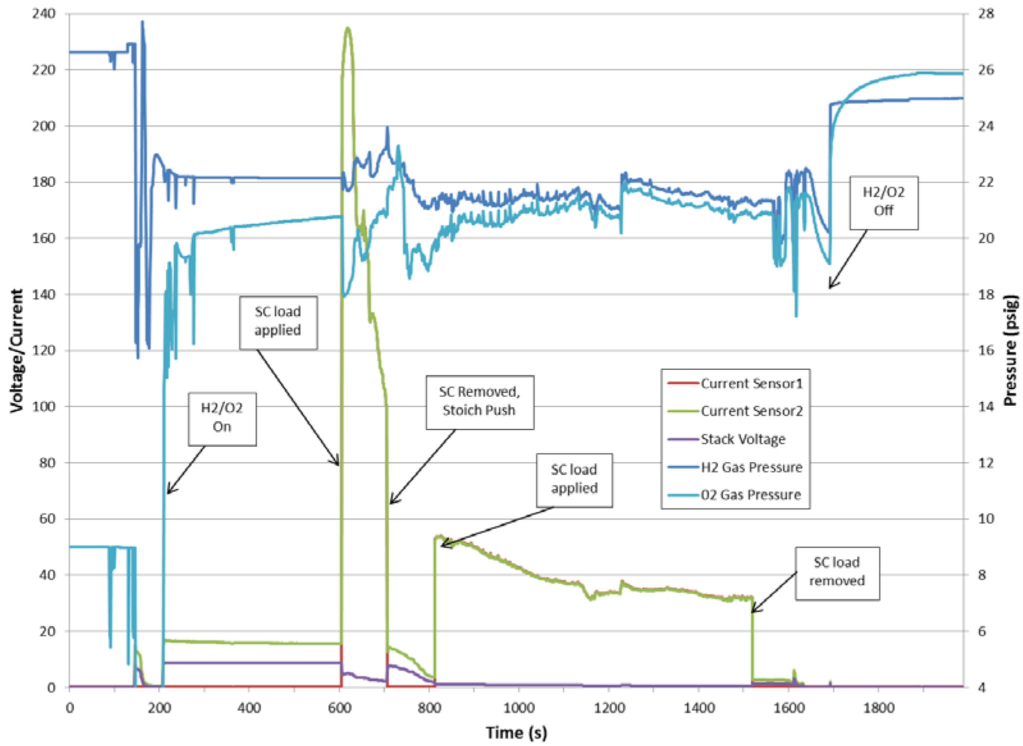

Figure 17. Short-circuit test–reactant gas pressures and stack voltage/current

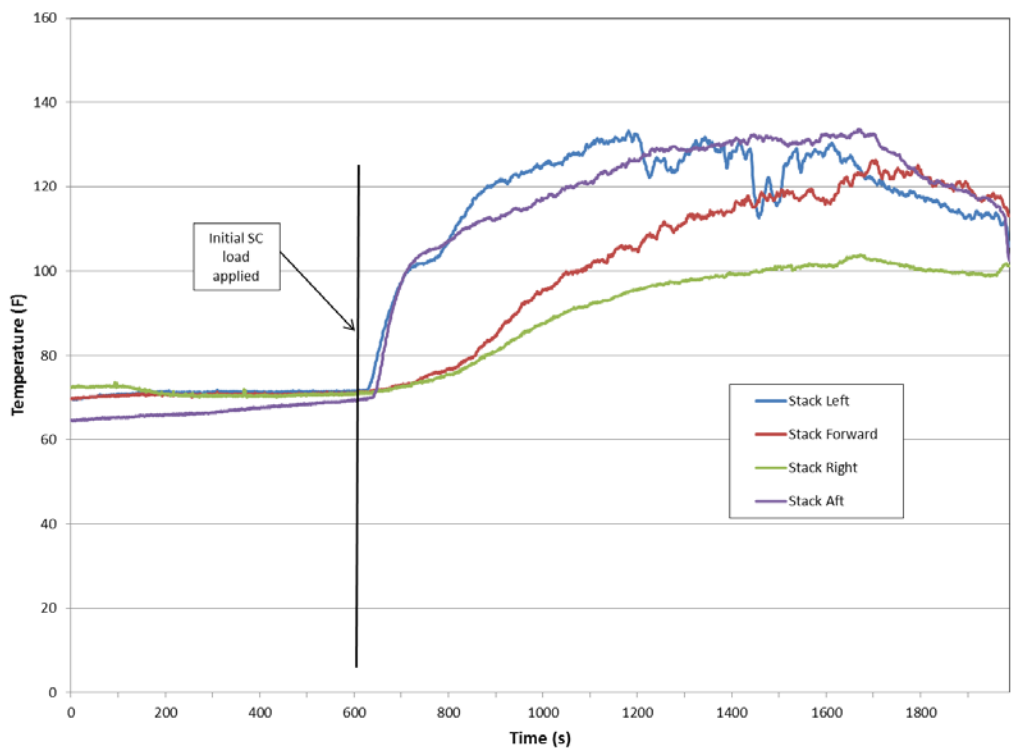

Figure 18. Short-circuit test–stack surface temperatures

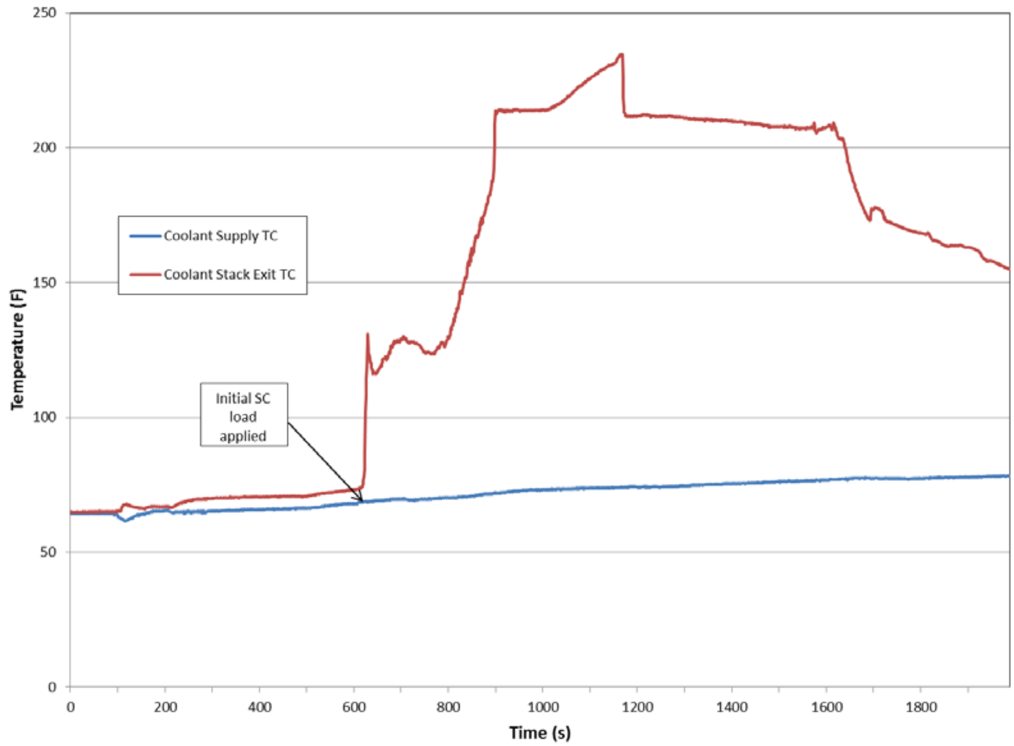

Figure 19. Short-circuit test–coolant supply and exit temperatures

The stack was run at the idle condition with a 15A load for a period of time before applying the short-circuit condition. Once applied, a peak current of 470A (235A/sensor) was observed for approximately 10 seconds. The voltage and current then began to drop significantly until reaching approximately 200A. At this point, the short-circuit condition was temporarily removed and gas pressures were adjusted in an attempt to recover full operation of the system. The current continued to drop during this duration and, approximately 100 seconds later, the short-circuit load was again applied. The stack was operated for nearly 12 minutes in this condition and, though the electrical capacity of the fuel cell continued to deteriorate, there were no observed conditions indicating a stack fire or hydrogen leakage in the chamber.

Temperature increases of the stack surfaces and coolant exit are shown in figures 18 and 19, respectively. These increases could be observed during the test as steam exiting the stack through the coolant exhaust ports located on top of the stack.

A post-test examination of the fuel cell stack showed little to no damage to the stack; however, during the post-test teardown of the stack, it showed significant internal damage. All of the MEAs were damaged, and some sections were destroyed. In addition, further evidence of the heat generated within the stack was seen in discolorization of the bipolar plates, damage to the gasket materials, and burnt components of the plastic frame surrounding each layer of the cell. The gasket material at both cathode inlet ports failed because of the heat damage, but this was of little consequence because the two ports only leaked into each other, causing no further damage. The damage to the bipolar plates was most severe toward the center of the stack and decayed in size toward the outer cells.

4.3 CROSSFLOW CONDITION TEST

Figures 20–24 show the results of the crossflow test. Figure 20 shows a plot of the stack voltage and current along with the supply H_2 and O_2 pressures for the crossflow test. Figure 21 shows the four stack surface temperatures, figure 22 shows the coolant supply and exit temperatures, and figure 23 shows the temperatures from the two temperature trees installed in the pressure vessel. Figure 24 shows the H_2 data from within the pressure vessel.

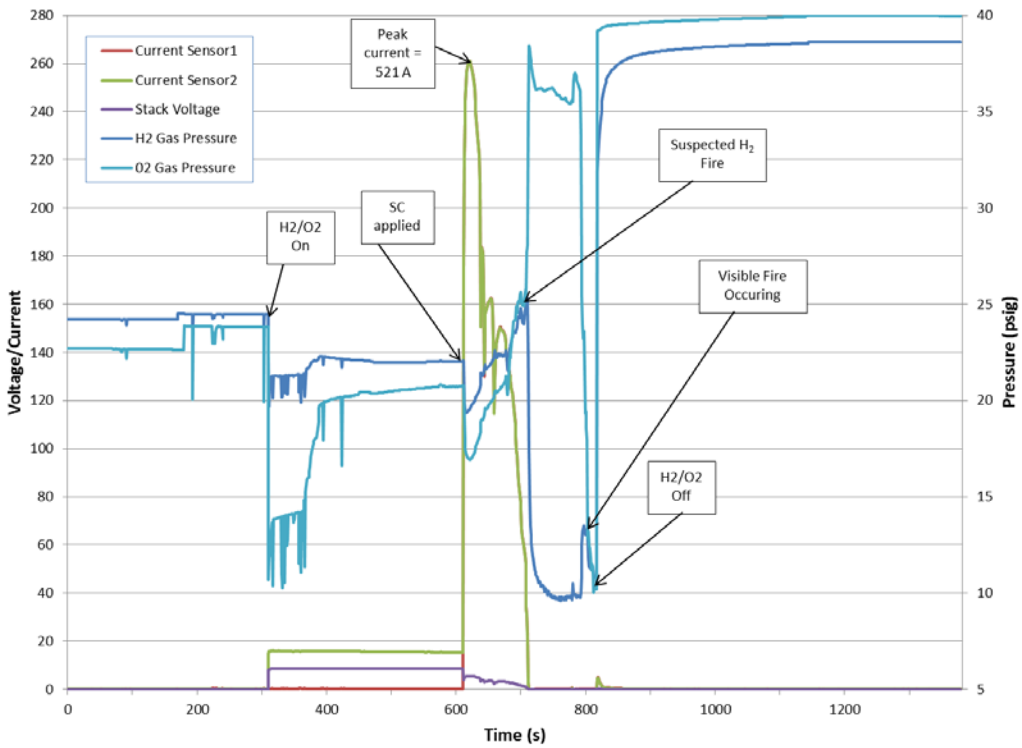

Figure 20. Crossflow condition test–reactant gas pressures and stack voltage/current

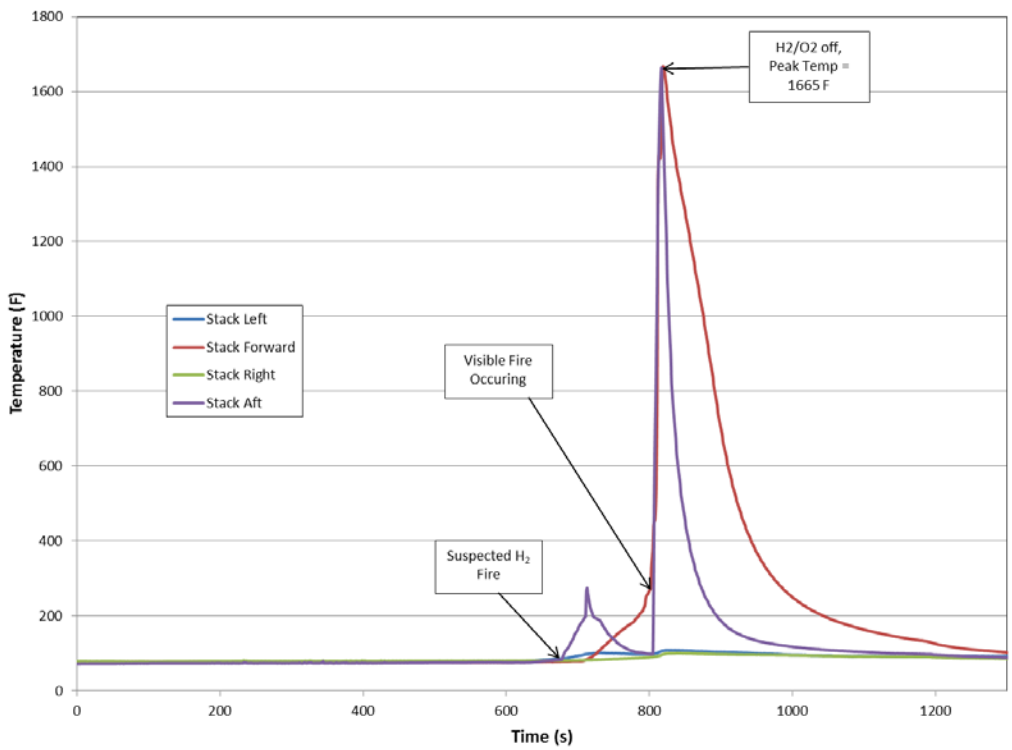

Figure 21. Crossflow condition test–stack surface temperatures

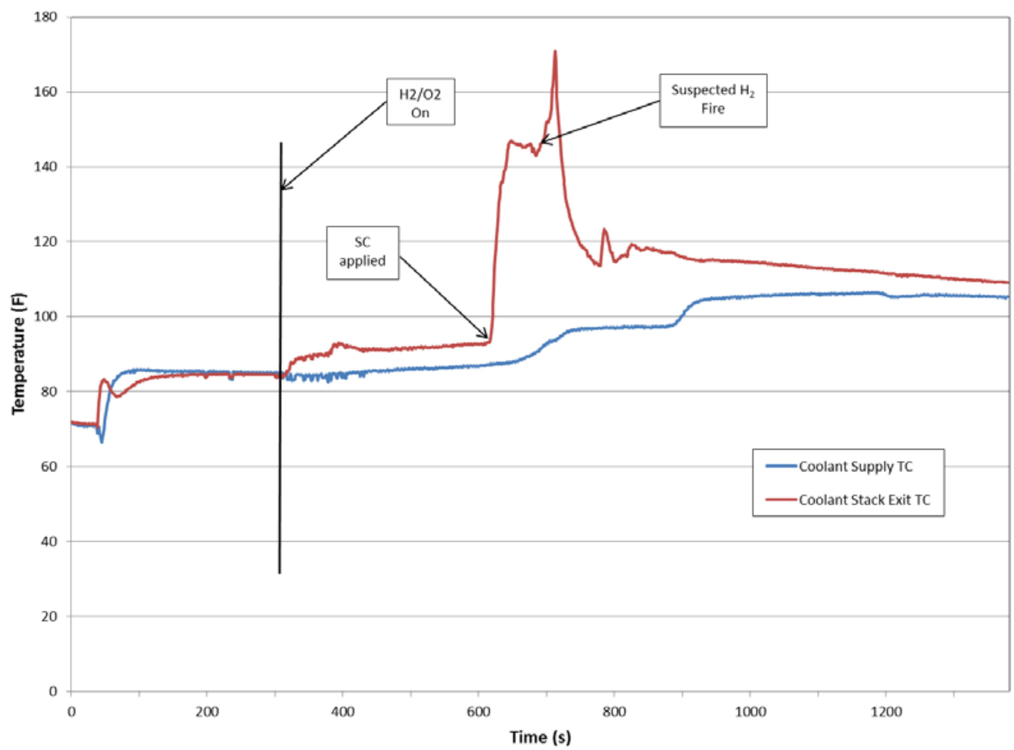

Figure 22. Crossflow condition test–coolant supply and exit temperatures

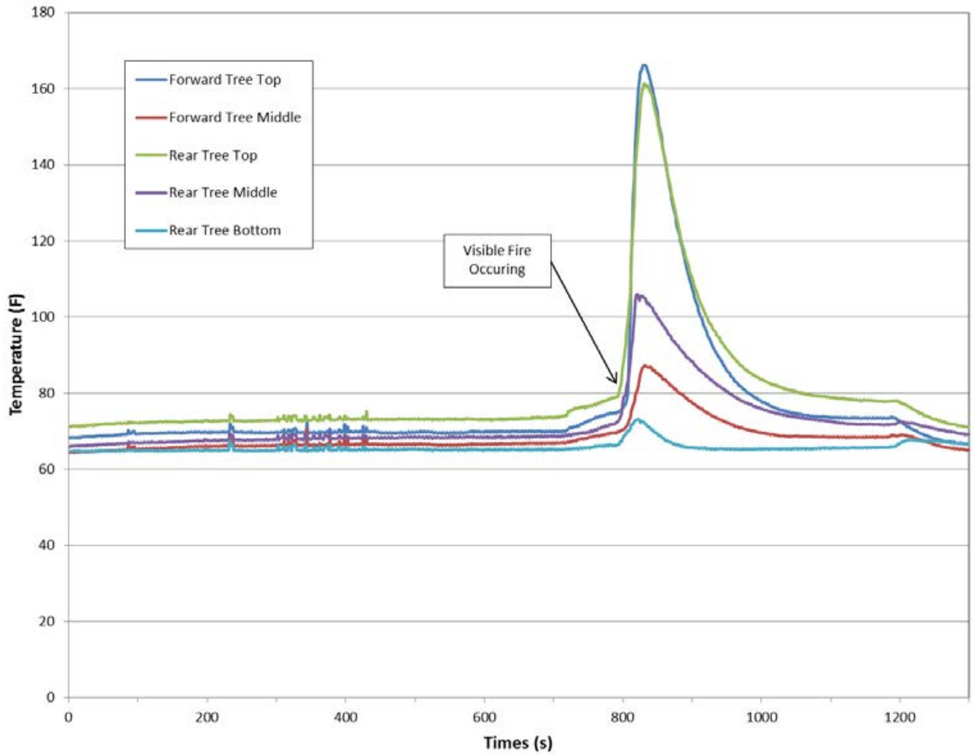

Figure 23. Crossflow condition test–pressure vessel temperatures

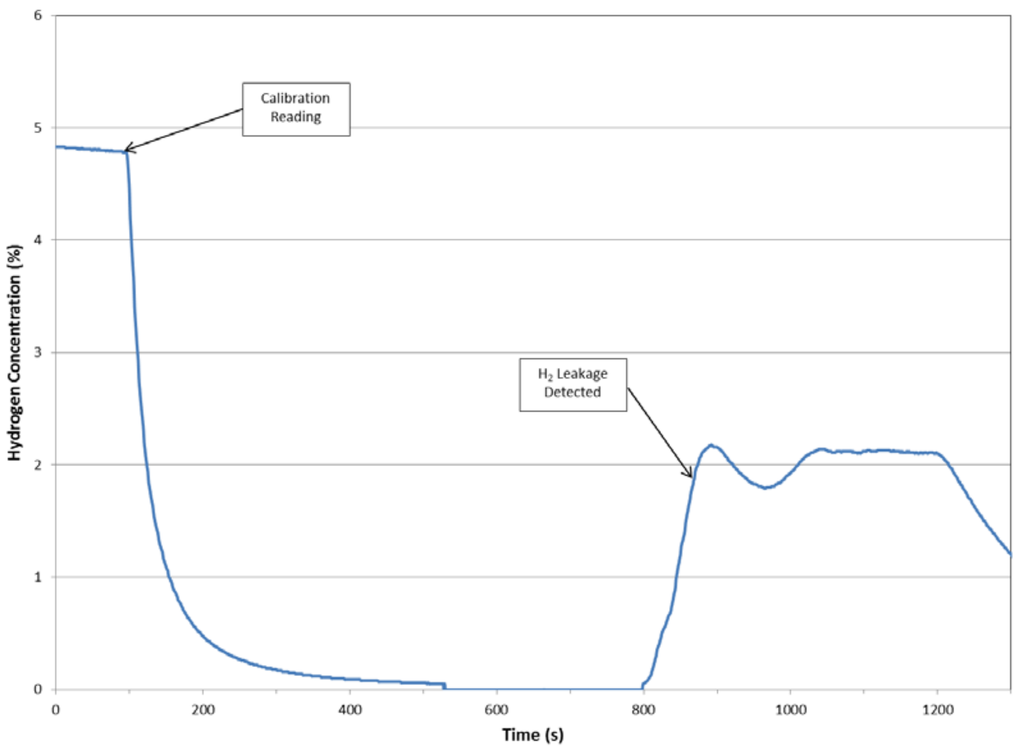

Figure 24. Crossflow condition test–hydrogen concentration

After supplying the reactant gases to the fuel cell, it is observed in figure 20 that, because of the crossover condition, there was initial difficulty in obtaining a constant gas pressure supply to the stack. Nevertheless, the stack was able to be operated in its idle condition at a load of 15A for a period of approximately 5 minutes without any apparent impact to the resulting voltage or current output of the stack. After approximately 5 minutes of idle performance, a short-circuit condition was applied to the fuel cell stack. This resulted in a peak current of 521A for approximately 4 seconds. The voltage and current then decayed until complete failure 110 seconds later. At the approximate time of the stack current reaching 0A, it is suspected the H_2 fire initiated. This suspicion regarding the timing of the H_2 fire is because of the pressure readings observed in figure 20 and the slight stack surface temperature (see figure 21) and pressure vessel temperature increases (see figure 23) observed at this time. In addition, figure 22 shows an increase in the coolant exit temperature at this time. Approximately 90 seconds later, a visible fire occurred along with the detection of H_2 leakage into the pressure vessel. At this point, the reactant gases were turned off and the fire rapidly self-extinguished.

A post-test evaluation of the fuel cell stack showed significant external damage. There was evidence of two distinct damage areas external to the fuel cell stack. The first, shown in figure 25, was at one of the O_2 outlet ports; the other was located at both of the O_2 inlet ports, as shown in figure 26.

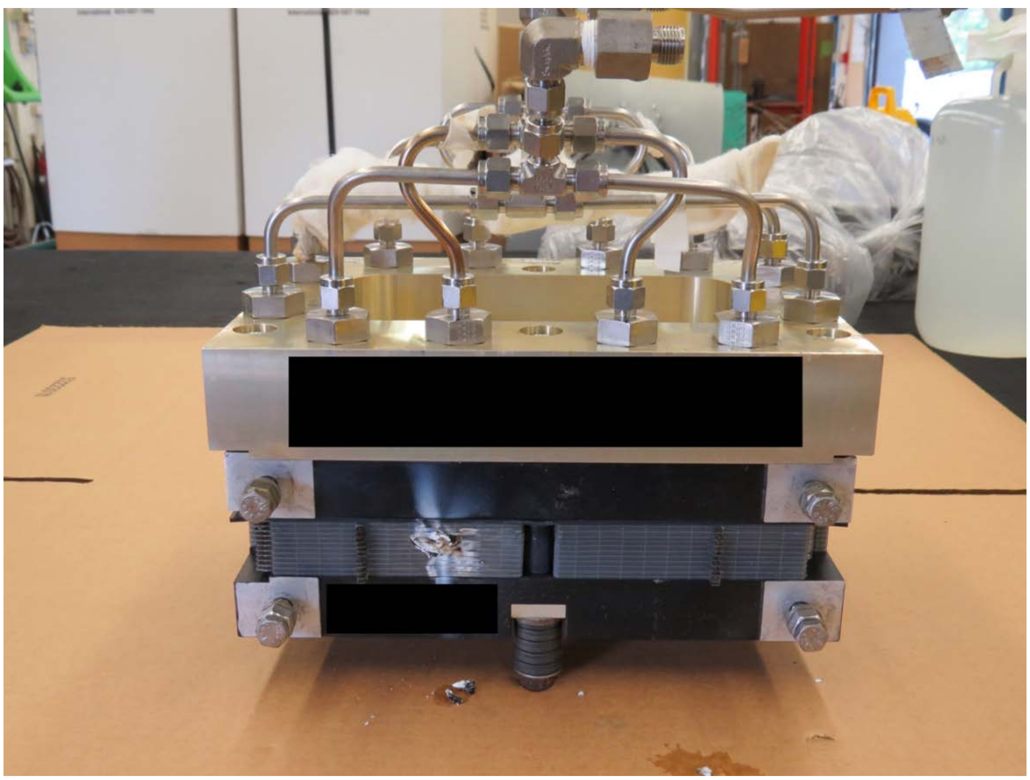

Figure 25. Crossflow condition test–external damage at O_2 outlet port

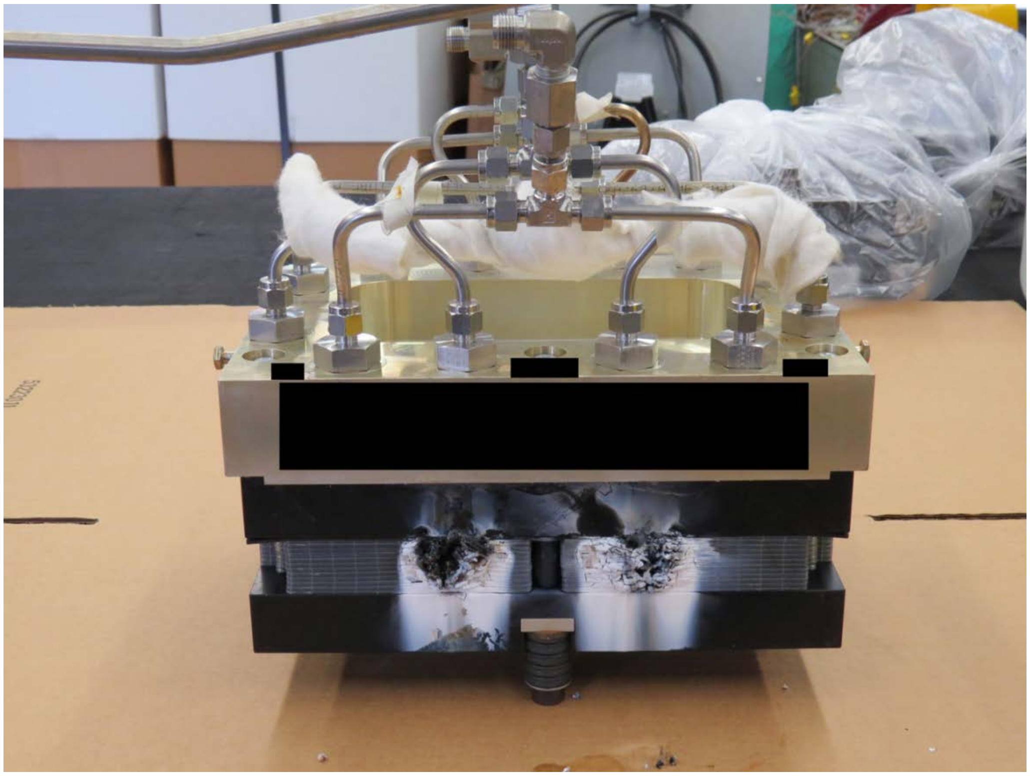

Figure 26. Crossflow condition test–external damage at O_2 inlet ports

During a complete teardown analysis of the stack, significant internal damage was observed. Nine of the ten cells were fused together, and a large hole was burned straight through the MEAS. Again, heavier signs of damage were observed toward the center of the stack. The gasket material and metal bipolar plate material between the O_2 manifold and ambient environment were destroyed by burning. Though the damage was severe, it still remained localized and did not appear to propagate throughout the active area of the cells. Photographs of the internal damage noted during the teardown analysis are shown in figure 27.

Figure 27. Crossflow condition test–internal damage to fuel cell stack

4.4 ADDITIONAL DATA—HYDROGEN LEAKAGE

During the first attempt at conducting the short-circuit condition test, there was an accidental failure of one of the anode gas connection points. This failure resulted in a hydrogen leak into the pressure vessel, which came very close to reaching the lower flammability limit. This constitutes another potential failure condition that could lead to hazardous conditions and must be protected against.

Figures 28–30 show the results from this failure condition. Figure 28 shows a plot of the stack voltage and current along with the supply H_2 and O_2 pressures. Figure 29 provides the surface temperatures for the four stacks, and figure 30 provides the H_2 data from within the pressure vessel.

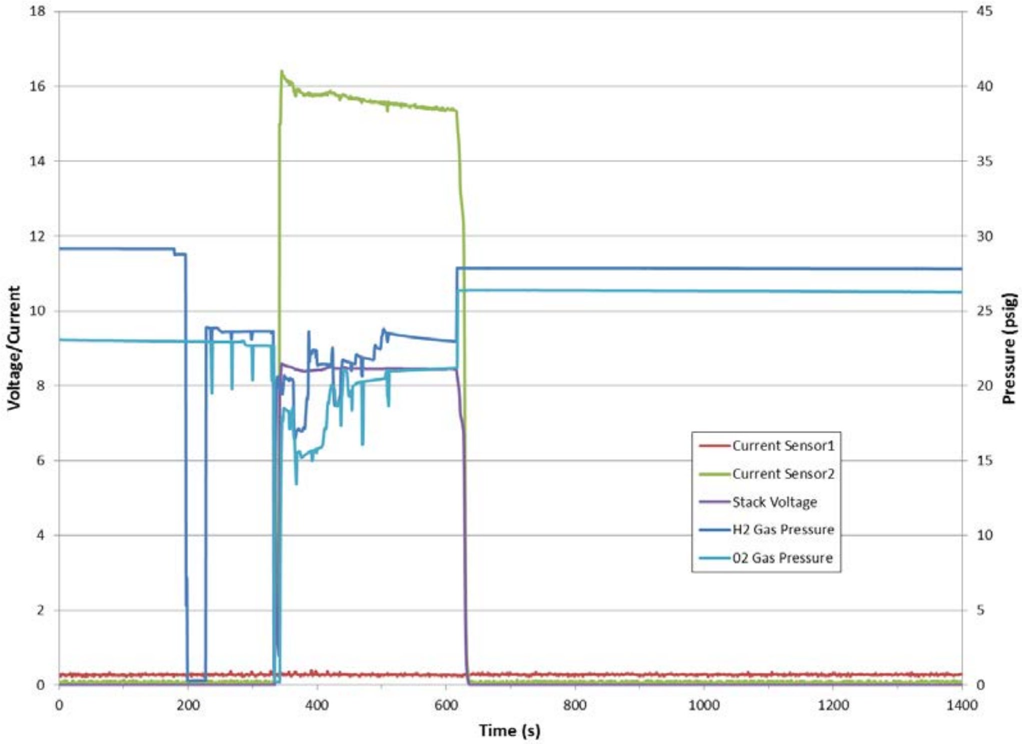

Figure 28. Hydrogen leakage–reactant gas pressures and stack voltage/current

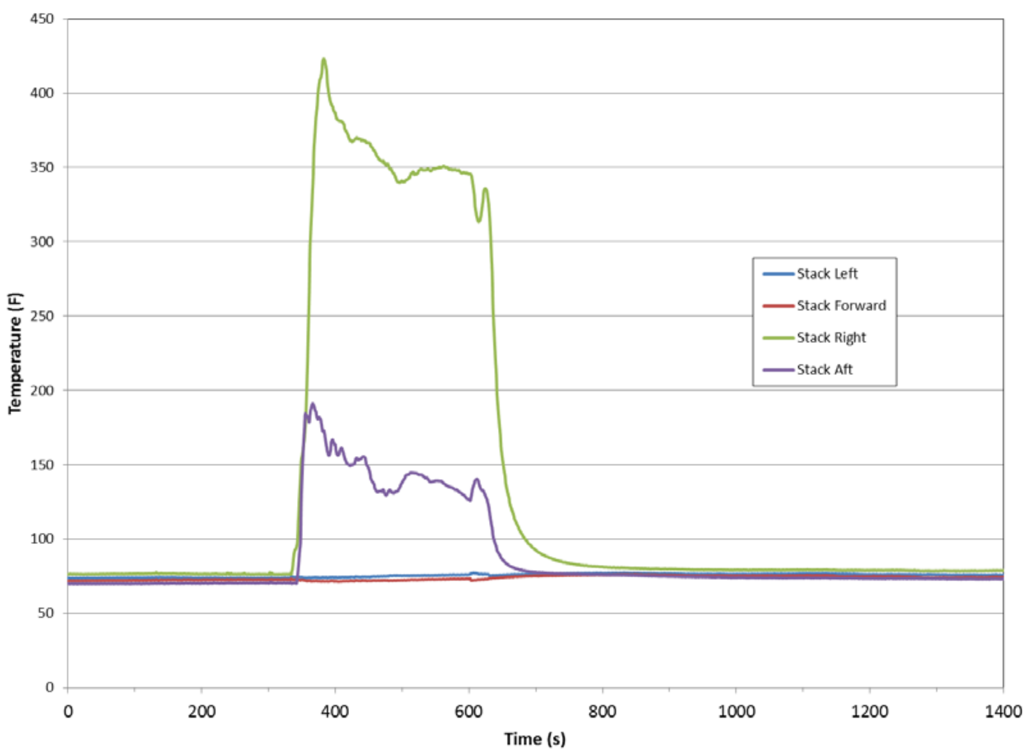

Figure 29. Hydrogen leakage–stack surface temperatures

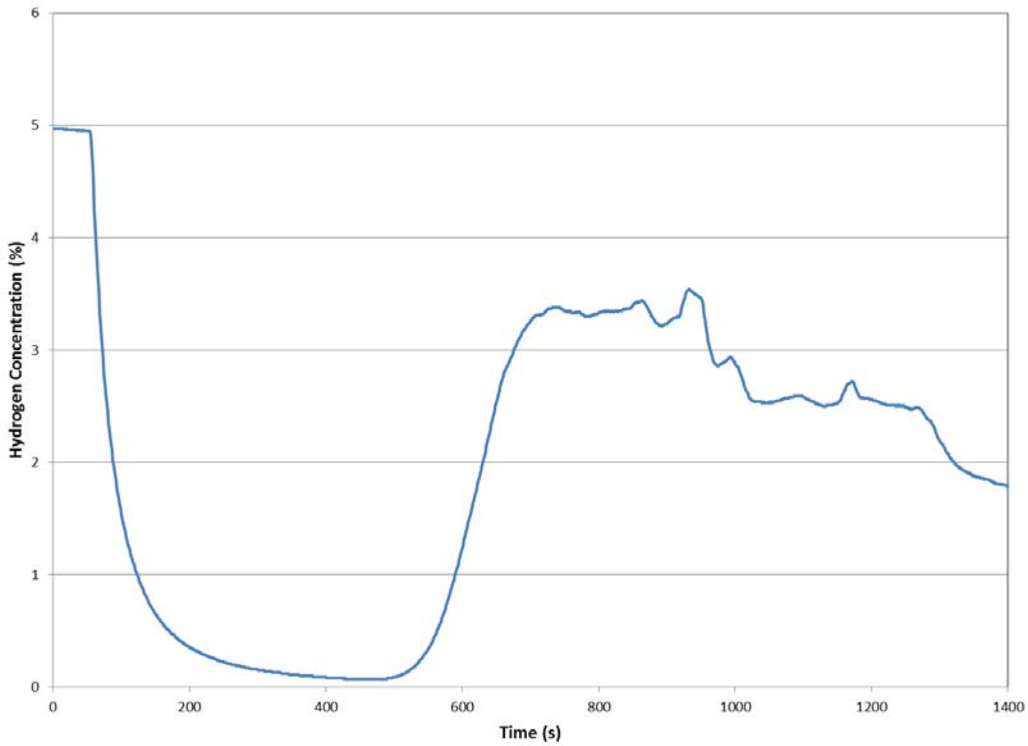

Figure 30. Hydrogen leakage–hydrogen concentration

Aside from the H_2 concentration reading in figure 30, there were several indicators that there was a failure condition existing within the stack. Figure 28 shows that the test operators were having a difficult time maintaining the reactant gas pressures. In hindsight, it is clear that this was due to the H_2 leak occurring at the time. In addition, stack surface temperatures indicated a failure condition long before the leak was detected by the gas analyzer, with temperatures exceeding 400°F. There were, however, no visual indications of any thermal event on the HD or FLIR video.

5. CONCLUSIONS

In collaboration with Parker Hannifin, the Fire Safety Branch of the FAA conducted testing to evaluate the effects of three potential failure conditions of hydrogen proton exchange (or polymer electrolyte) membrane fuel cell stacks supplied by Nuvera Fuel Cells. The three conditions examined were a loss of coolant to the stack, short circuit, and a crossflow condition. After exposing the stack to the various failure conditions, it was observed that the stack continued to operate for an extended period of time before any hazardous effects were observed. Because the fuel cell stack was not expected to survive as long as it did, the typical balance of plant to properly condition the supply gases was not utilized. Had these gases been properly conditioned, an increased survivability of the stack would be expected.

Once the stack components failed, external heat in excess of the normal operational temperature was observed; however, only the loss of coolant and crossflow tests resulted in any fire/sparking from the test unit. The crossflow condition test resulted in hydrogen leakage into the surrounding pressure vessel.

There were various opportunities for detection of the failure during the time from when the failure event was initiated to when the stack deteriorated, and finally when the point of flaming/sparking began. Failure detection could have been achieved by monitoring the reactant gas supply pressures, coolant exit temperatures, stack surface temperatures, or the stack output voltage and current.

An additional failure mechanism was observed during testing when one of the hydrogen gas connections failed, resulting in a large leak of hydrogen into the surrounding vessel. Though this leak approached the lower explosive limit, there was ample opportunity for the failure to have been detected. The failure could have been noted via monitoring of the gas supply pressures or stack surface temperatures.

The testing showed that the stacks were extremely robust under a variety of failure conditions and that, with proper monitoring of key variables, the failures could have been detected and flow of reactant gases stopped prior to any hazardous effects occurring. It is recommended that any installation of a hydrogen fuel cell system ensure that reactant supply gas pressures, stack temperatures, coolant temperatures, and stack electrical load characteristics be adequately monitored and connected to system shutdown features. In addition, provisions should be made so that the surrounding environment is monitored for any temperature or hydrogen gas concentration increases.

It should be noted that this testing only evaluated failure mechanisms of the fuel cell stack itself. The storage and distribution of high-pressure hydrogen gas provides its own level of hazard that additionally needs to be addressed. Further testing of other hydrogen fuel cells, with a focus on these aspects, should be conducted and evaluated prior to any implementation of a fuel cell system to ensure that all safety issues are adequately addressed.

6. REFERENCES

1. “Membrane Electrode Assembly - Electro-Chemical Reaction Diagram,” by CFA213FCE - Own work. Licensed under CC BY-SA 3.0 via Commons, available at https://commons.wikimedia.org/wiki/File:Membrane_Electrode_Assembly_-_Electro-Chemical_Reaction_Diagram.jpg#/media/File:Membrane_Electrode_Assembly_-_Electro-Chemical_Reaction_Diagram.jpg (accessed 03/02/16).